First hitting time and option pricing problem under Geometric Brownian motion with singular volatility

HAOYAN ZHANG, YECE ZHOU, XUAN LI, YINYIN WU*
College of Science,
Civil Aviation University of China,
Tianjin 300300,
CHINA

**Corresponding Author*

Abstract: In this paper, we discuss the first hitting time and option pricing problem under Geometric Brownian motion with singular volatility. By solving the Sturm-Liouville equation and introducing probability scheme, we derive the closed-form solutions to the target problems. At last, numerical results are provided to analyze our calculations.

Key-Words: Geometric Brownian motion, First hitting time, Laplace transform, Option pricing, Closed-form solution, Numerical result

Received: July 15, 2023. Revised: October 14, 2023. Accepted: October 29, 2023. Published: November 22, 2023.

1 Introduction

Geometric Brownian motion (GBM) is a simple continuous-time stochastic process in which the logarithm of the randomly varying quantity of interest follows a Brownian motion with drift and a special case of Markov process. Geometric Brownian motion frequently features in mathematical modeling. The advantage of considering this process lies in its universality, as it represents an attractor of more complex models that exhibit non-ergodic dynamics, we refer the readers to [1], [2], [3]. Geometric Brownian motion is defined by $\frac{dS_t}{S_t} = \mu dt + \sigma dW_t$, where μ is a drift term, σ is a noise amplitude, and W_t is a Wiener process. [4] proposed this model without the noise, i.e. $\sigma = 0$, that means the model is simply exponential growth at rate μ. If $\sigma \neq 0$, it can be interpreted as exponential growth with a fluctuating growth rate. [5] put forward the logarithm of random variables satisfying Geometric Brownian motion. The main factors affecting the change of stock price are the rising trend of stock price over time and the average volatility of stock price. The contribution of the former to the growth of stock prices relies on the length of time; the latter only depends on the random fluctuations caused by Brownian motion. In the classical Wiener process, we assume that the expected drift rate is constant, that is, $\mu(\cdot) = \mu$. Therefore, Geometric Brownian motion, a widely used model to describe the behavior of stock prices, is obtained. If the price of the stock at time t is S, then the drift rate of the underlying model should be μS, where μ is a constant. But in practice, it is more reasonable to assume that the expected rate of return is not constant. Compared with Brownian motion, the expectation of Geometric Brownian motion is independent of the stock price, which conforms to the expectation of real market.

In recent years, Geometric Brownian motion has been widely used in the field of transportation planning in [6] and management in [7]. See, for instance that, [8] predicted traffic flow. [9] predicted a minimum future closing price in a company by using GBM. Among others, Geometric Brownian motion has applications in ecology in [10], economics in [11], [12], etc. More recent work on option pricing problems, readers may consult the papers in [13], [14], [15], [16], [17].

In the financial field, Geometric Brownian motion is the most widely used dynamic. In 1965, based on Einstein's Brownian motion research method and Wiener's definition of Brownian motion, [18] established a Geometric Brownian motion model to describe the random fluctuation of stock prices. In 1973, [19] first assumed that the stock price was subject to the Geometric Brownian motion model of Samuelson, to deduce the famous B-S option pricing formula, and used the stock price model to solve the reasonable pricing problem of financial derivatives such as stocks, bonds, currencies and commodities. In the same year, [20] also derived the B-S option pricing formula using the stochastic calculus method, further weakened the assumptions on which the B-S option pricing formula depends, and added the Poisson jump process to the Geometric Brownian motion model, expanding the application scope of the B-S option pricing formula. Later in [21], the paper put forward a simple

and efficient numerical procedure for valuing options for which premature exercise may be optimal. Also in [22], the paper empirically provided an alternative pption pricing models by first deriving an option model that allows volatility, interest rates and jumps to be stochastic. Further, [23] provided an analytical treatment of a class of transforms, including various Laplace and Fourier transforms as special cases, that allow an analytical treatment of a range of valuation and econometric problems to solve example applications including fixed-income pricing models, with a role for intensity-based models of default, as well as a wide range of option-pricing applications. It is well known that the volatility and yield are set as constants in the Geometric Brownian motion. Economists often used this Geometric Brownian motion to describe the stock trend, so it is very meaningful to study it. In addition, this has attracted the attention and discussion of a large number of scholars. Among them, it is an important aspect to analyze asset pricing with the change of financial time series. [24] considered the research of multivariate GARCH model in explaining the difference in expected returns between Shanghai and Shenzhen of China's stock market. In addition, the difference is not remarkable. Therefore, this paper mainly focuses on the option price under the Geometric Brownian motion process. However, because the classical assumption is too idealistic, it has obvious limitations, that is, the volatility and yield in the actual market do not meet the constant assumption. For example, Figure 1 & Figure 2 show the trend of the Dow Jones Industrial Index and the United States Federal Fund Interest Rate (1955-2023). It is obvious

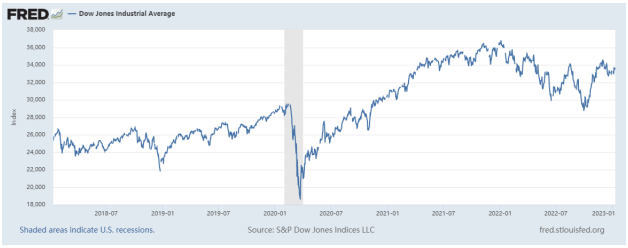

Fig. 1: Dow Jones Industrial Index from 2018-2023

that the volatility and yield are not constant, and they will change under various influences. If we consider the case of random volatility, in most cases, we cannot give a closed-form solution and must define the appropriate distribution for the volatility. For example, [25] considering the pricing of derivative options with random volatility, only provided the pricing formula, and did not give a closed-form solution. Hence, this paper take the broken drift and singular volatility into consideration.

The first hitting time is a mathematical term that

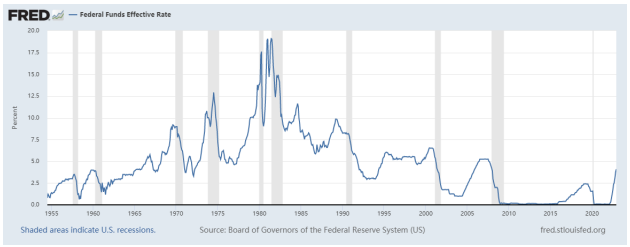

Fig. 2: The United States Federal Fund Interest Rate from 1955-2023

represents the moment when a stochastic process first reaches a certain set of states. In terms of application, the first hitting time has important practical significance, for example, in fields like financial risk management, communication network optimization, and transportation scheduling. In addition, the first hitting time can also be used for the optimization of prediction models and algorithms, for example in fields like machine learning and data mining. By understanding the nature and calculation methods of the hitting time, we can better understand and optimize the behavior of stochastic processes, thereby providing better solutions for practical applications. On one hand, the first hitting time problem is very crucial as a classic subject. On the other hand, the study of the first hitting time problem of Geometric Brownian motion with broken drift and singular volatility is very few at present. We also view this problem as our target study. Around the literature about the first hitting time problems, the authors may consult [26] under skew CIR process, [27] under regime switching Geometric Brownian motion, [28] under sticky skew Brownian motion, and [29] under sticky skew CIR process. A most recent paper in 2019, [30] considered the optimal stopping and first hitting time problems of Brownian motion with broken drift. However, there exists few papers concerning on hitting time and option pricing problems by introducing singularity coefficients. In addition, traditional methods when solving the pricing problem needs complex calculations or numerical scheme. Complex calculations may result in inaccurate or even non-closed-form solutions. Numerical computations have high requirements for accuracy and real-time performance of the results. Therefore, this paper tries to solve the first hitting time and option pricing problem under our setting model, respectively. In probability scheme, we only need to employee the variable substitution and probability distribution of random variable function for our target under risk-neutral measure. Now let us introduce the Geometric Brownian motion with broken drift and

singular volatility by

$$\frac{dS_t}{S_t} = \mu(S_t)dt + \sigma(S_t)dW_t, \tag{1}$$

where

$$\mu(S_t) = \begin{cases} \mu_1, & S_t \geq a, \\ \mu_2, & S_t < a, \end{cases} \sigma(S_t) = \begin{cases} \sigma_1, & S_t \geq a, \\ \sigma_2, & S_t < a. \end{cases}$$

The notations μ_1 and μ_2 are the drifts, σ_1 and σ_2 are the volatilities, a is the singularity boundary, S_t is the stock price at time t and W_t is a standard Brownian motion. When we consider the option pricing problem, in traditional option pricing theory, we always assume the drift term to be the risk-free interest rate r, this model (1) reduces to

$$\frac{dS_t}{S_t} = rdt + \sigma(S_t)dW_t. \tag{2}$$

Before proceeding the study, please let us retell our target problem. In this paper, we consider the Laplace transform of the first hitting time and option pricing problem under Geometric Brownian motion with singular volatility, respectively. To get the Laplace transform of first hitting time under the above model, we should solve the Sturm-Liouville equation, and when facing the option pricing problem, we apply the probability scheme to calculate this object. All the results we get are closed-form. At last, we provide the numerical results to explain some interesting phenomena under different coefficients.

The rest of this paper is organized as follows. Section 2 analyzes the option pricing problem under Geometric Brownian motion with singular volatility and use Matlab to get numerical results. Under our model the Laplace transform of first hitting time and the theoretical and numerical results are respectively calculated in Section 3. Section 4 concludes this paper and explains some future study.

2 Option Pricing

2.1 Theoretical results

Let us assume that $(\Omega, \mathcal{F}, \mathbf{P})$ is a complete probability space, $\mathcal{F}$ is a σ-algebra on Ω and $\mathbf{P}$ represents a probability measure of $(\Omega, \mathcal{F})$. In this paper, we consider that the underlying asset satisfies (2).

We can write the definition of the option price under risk-neutral measure by:

$$f(t, S_t) = e^{-r(T-t)}\mathbb{E}^{\mathbf{Q}}[max(S_T - K)^+], \tag{3}$$

where K is the exercise price and T is the maturity date.

Next, we naturally draw the theorem of option pricing:

Theorem 1. *If the stock price satisfies the Geometric Brownian motion with risk-free interest rate and singular volatility in (2), then the option price defined by (3) takes the form of:*

$$f(t, S_t) = \begin{cases} S_t\Phi(\frac{ln\frac{S_t}{K} + (r + \frac{1}{2}\sigma_1^2)(T-t)}{\sigma_1\sqrt{T-t}}) - \\ Ke^{-r(T-t)}\Phi(\frac{ln\frac{S_t}{K} + (r - \frac{1}{2}\sigma_1^2)(T-t)}{\sigma_1\sqrt{T-t}}), \\ S_t \geq a, \\ S_t\Phi(\frac{ln\frac{S_t}{K} + (r + \frac{1}{2}\sigma_2^2)(T-t)}{\sigma_2\sqrt{T-t}}) - \\ Ke^{-r(T-t)}\Phi(\frac{ln\frac{S_t}{K} + (r - \frac{1}{2}\sigma_2^2)(T-t)}{\sigma_2\sqrt{T-t}}), \\ S_t < a. \end{cases}$$

Proof. According to Itô's formula:

$$df(t, S_t) = (\frac{\partial f}{\partial t} + \frac{\partial f}{\partial S_t}\mu S_t + \frac{1}{2}\frac{\partial^2 f}{\partial t^2}\sigma^2 {S_t}^2)dt \tag{4}$$

$$+ \frac{\partial f}{\partial S_t}\sigma S_t dW_t. \tag{5}$$

Let $lnS_t = G_t$, then we have $\frac{\partial G_t}{\partial S_t} = \frac{1}{S_t}$, $\frac{\partial^2 G_t}{\partial {S_t}^2} = -\frac{1}{{S_t}^2}$ and $\frac{\partial G}{\partial t} = 0$.
We recall (5), getting

$$dG_t = dlnS_t = (\mu - \frac{\sigma^2}{2})dt + \sigma dW_t.$$

Further, we get

$$lnS_T \sim N(lnS_t + (\mu - \frac{\sigma^2}{2})(T-t), \sigma^2(T-t)).$$

Letting $m = lnS_t + (\mu - \frac{\sigma^2}{2})(T-t)$, $s = \sigma\sqrt{T-t}$ and applying the probability scheme, we have

$$\begin{aligned} &\mathbb{E}^{\mathbf{Q}}[max(S_T - K)^+] \\ &= \int_K^\infty (S_t - K)f(S_t)dS_t \\ &= \int_{lnK}^\infty (e^{lnS_t} - K)g(lnS_t)d(lnS_t) \\ &= \int_{\frac{lnK-m}{s}}^\infty [e^{(sw+m)} - K]h(w)dw \\ &= \int_{\frac{lnK-m}{s}}^\infty e^{(sw+m)}(2\pi)^{-\frac{1}{2}}e^{(\frac{-w^2}{2})}dw - K\Phi(\frac{m - lnK}{s}) \\ &= e^{(\frac{s^2}{2}+m)}\int_{\frac{lnK-m}{s}}^\infty (2\pi)^{-\frac{1}{2}}e^{\frac{-(w-s)^2}{2}}dw - K\Phi(\frac{m - lnK}{s}) \\ &= e^{(\frac{s^2}{2}+m)}\Phi(s - \frac{lnK - m}{s}) - K\Phi(\frac{m - lnK}{s}), \end{aligned}$$

where $f(S_t)$ is the density function of S_t, $g(lnS_t)$ is

the density function of lnS_t, $h(\cdot)$ is the standard normal density function and lnK obeys normal distribution that the mean is m and the standard deviation is s, that is $lnK \sim N(m, s^2)$.

Therefore, we apply the result to (3), acquiring

$$f(t,S_t) = e^{-r(T-t)}[e^{\frac{s^2}{2}+m}\Phi(s-\frac{lnK-m}{s}) - K\Phi(\frac{m-lnK}{s})],$$

where

$$\begin{aligned} s-\frac{lnK-m}{s} &= \frac{\sigma^2(T-t)+lnS_t/K+(r+\frac{1}{2}\sigma^2)(T-t)}{\sigma\sqrt{T-t}} \\ &= \frac{ln(\frac{S_t}{K})+(r+\frac{1}{2}\sigma^2)(T-t)}{\sigma\sqrt{T-t}} = d1, \\ \frac{m-lnK}{s} &= \frac{lnS_t+(r-\frac{1}{2}\sigma^2)(T-t)-lnK}{\sigma\sqrt{T-t}} \\ &= \frac{ln(\frac{S_t}{K})+(r-\frac{1}{2}\sigma^2)(T-t)}{\sigma\sqrt{T-t}} = d2, \end{aligned}$$

and

$$\begin{aligned} m+\frac{s^2}{2} &= lnS_t+(r-0.5r^2)(T-t)+\frac{\sigma^2(T-t)}{2} \\ &= lnS_t+r(T-t). \end{aligned}$$

Finally, we replace μ and σ by r and $\sigma(\cdot)$, which finishes our proof. □

2.2 Numerical results

We use Matlab for numerical simulation to realize the trend and comparison of option prices and stock prices. In our setting, we choose a to be close to the median value of 7 and $r = 0.1$. When the stock price S_t is greater than or equal to 7, we take volatility σ as 1.8, and when S_t is less than 7, we take volatility σ as 1.2. Because risk in markets is usually high, implying that the greater the risk is, the greater the potential gain gets, but the greater the potential loss happens. Therefore, the higher the stock price is, the more severe the fall is likely to be; while the lower the stock price is, the less room for further decline the stock price is. More precisely, we set

$$a = 7, r = 0.1, \sigma(t) = \begin{cases} 1.8, & S_t \geq a, \\ 1.2. & S_t < a. \end{cases}$$

Figure 3 is the results of our numerical simulation. It can be seen from Figure 3 that the cumulative value of derivatives has existed for a long time due to the continuous compounding of stocks, so the overall trend is upward.

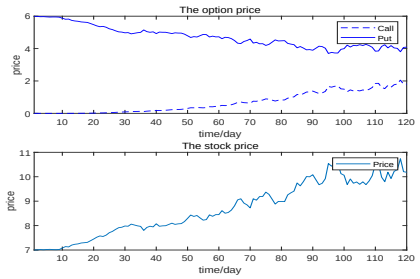

Fig. 3: The trend and comparison of option prices and stock prices

We observe the changes of option prices and stock prices by different parameters. First, fix broken boundary a and volatility σ, and change the value of r. The specific values are as follows:

$$a = 7, r = 0.2, \sigma(t) = \begin{cases} 1.8, & S_t \geq a, \\ 1.2, & S_t < a. \end{cases}$$

$$a = 7, r = 0.05, \sigma(t) = \begin{cases} 1.8, & S_t \geq a, \\ 1.2, & S_t < a. \end{cases}$$

It can be seen from Figure 4 & Figure 5 that blue curve is bigger than the red (green) curve. With the change of r value, both stock price and option price will change, in which the price of stock price and call option increases relative with the increase of value, which reflects the fact that the great r pushes the high level for stock price and the corresponding call option price.

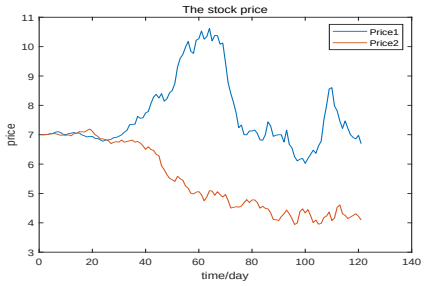

Fig. 4: The stock price and call option price with different r. The blue line relies on $r = 0.2$ and the red line relies on $r = 0.05$, respectively.

Moreover, we get the intuition that the change of σ has an effect on the price of the stock and the relative size of the impact of the yield on the price trend. Therefore, by changing the value of σ, the influences of different parameters on the stock price and option price are compared. Hence we fix broken boundary a

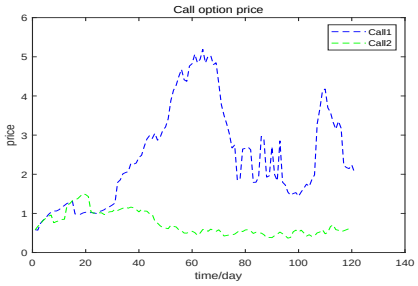

Fig. 5: The stock price and call option price with different r. The blue line relies on $r = 0.2$ and the green line relies on $r = 0.05$, respectively.

and r, and change the volatility value of σ. The specific values are as follows:

$$a = 7, r = 0.05, \sigma(t) = \begin{cases} 1.8, & S_t \geq a, \\ 1.2, & S_t < a. \end{cases}$$

$$a = 7, r = 0.05, \sigma(t) = \begin{cases} 2, & S_t \geq a, \\ 1.2, & S_t < a. \end{cases}$$

It can be seen from the Figure 6 & Figure 7 that blue curve is bigger than the red (green) color curve. When the value changes, the price of stock and option will also change. The price of stock and call option increases with the increase of σ value, which may explain that the great σ, leading high reward, pushes the high level for stock price and the corresponding call option price. We can also observe that the impact of r value on option prices is smaller than that of σ value, that is, the impact of volatility on asset prices is greater than that of yield. In our opinion, managing risk is far more important than guaranteeing expectation.

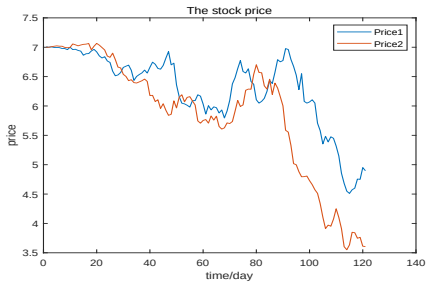

Fig. 6: The stock price under GBM with risk-free interest rate. The red line relies on $\sigma_1 = 1.8$ and $\sigma_2 = 1.2$ and the blue line relies on $\sigma_1 = 2$ and $\sigma_2 = 1.2$, respectively.

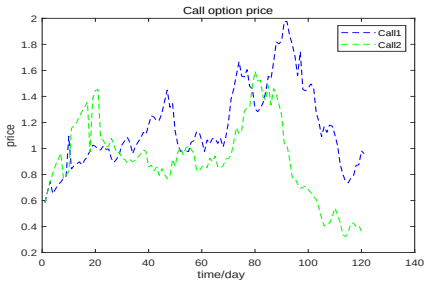

Fig. 7: Call option price under GBM with risk-free interest rate. The green line relies on $\sigma_1 = 1.8$ and $\sigma_2 = 1.2$ and the blue line relies on $\sigma_1 = 2$ and $\sigma_2 = 1.2$, respectively.

3 Laplace transform of first hitting time

3.1 Main results regarding first hitting time

First hitting time is the moment when a random variable passes a given threshold for the first time. For example, random walks leave a given space for the first time. It can also be diffusion limited reactions, polymer ring formation, stock market price dynamics, search problems, etc. The problem of lead-time is an important part of stochastic process theory. Stochastic process is the fundamental theory in financial mathematics, so the problem of first hitting time also plays an important role in financial mathematics.

In the study of financial markets, especially the pricing and risk management of path-dependent financial derivatives, the problem of first hitting time is almost always encountered. It is necessary to understand the distribution of first hitting time. However, it is not easy to obtain the distribution of the first hitting time directly, so some scholars obtained the distribution of the first hitting time by studying the Laplace transform of the first hitting time. More precisely, if we set the density function of the first hitting time to be $f(t)$, then the Laplace transform of the first hitting time is defined by

$$L(\lambda; x; l) = E_x[\exp(-\lambda\tau_l)] = \int_0^{+\infty} f(t)e^{-\lambda t}dt,$$

. By inverse Laplace transform,

$$f(t) = \frac{1}{2\pi j}\int_{\lambda-j\infty}^{\lambda+j\infty} L(\lambda; x; l)e^{\lambda t}dt,$$

we get the density function of the first hitting time.

As the first hitting time problem is an important subject in optimal stopping, the first hitting time problem of Geometric Brownian motion with broken drift term is studied next. Then, set a constant level $l \geq 0$

and define the first hitting time of X for touching l by $\tau_l = inf\{t \geq 0; X_t = l\}$. The Laplace transform of τ_l is $L(\lambda; x; l) = E_x[\exp(-\lambda\tau_l)]$, where $X_0 = x$ is the initial point of X and λ is a parameter. Next lemma provides the main result under Geometric Brownian motion about the Laplace transform of the first hitting time, the proof can be seen in Borodin and Salminen.

Theorem 2. *(Lemma in [31]) If X_t is the Geometric Brownian motion, then the Laplace transform of first hitting time of X for touching l is expressed by*

$$L(\lambda; x; l) = E_x[\exp(-\lambda\tau_l)] = \frac{f(x)}{f(l)},$$

where

$$f(x) = x^{r_1} + x^{r_2}$$

and

$$r_1 = \frac{(1 - \frac{2\mu}{\sigma^2}) + \sqrt{(\frac{2\mu}{\sigma^2} - 1)^2 + \frac{8\lambda}{\sigma^2}}}{2},$$
$$r_2 = \frac{(1 - \frac{2\mu}{\sigma^2}) - \sqrt{(\frac{2\mu}{\sigma^2} - 1)^2 + \frac{8\lambda}{\sigma^2}}}{2}.$$

Further we consider the first hitting level l under Geometric Brownian motion with broken drift and singular volatility, this immediately leads to the following theorem.

Theorem 3. *If X_t is the Geometric Brownian motion with broken drift and singular volatility, then the solution to the S-L equation is expressed by*
Case 1: if $x \geq l$,

$$\begin{cases} f(x) = x^{r_{12}}, & l > x \geq a, \\ c_1 x^{r_{11}} + c_2 x^{r_{12}}, & a < x < l. \end{cases} \tag{6}$$

Case 2:if $x < l$,

$$\begin{cases} f(x) = x^{r_{21}}, & x > l \geq a, \\ b_1 x^{r_{12}} + b_2 x^{r_{22}}, & l < a < x. \end{cases} \tag{7}$$

where

$$c_1 = \frac{a^{r^{12}}(r^{21} - r^{12})}{a^{r^{11}}(r^{21} - r^{11})}, c_2 = \frac{a^{r^{12}}(r^{12} - r^{11})}{a^{r^{21}}(r^{21} - r^{11})},$$
$$b_1 = \frac{a^{r^{21}}(r^{22} - r^{21})}{a^{r^{12}}(r^{22} - r^{12})}, b_2 = \frac{a^{r^{21}}(r^{21} - r^{12})}{a^{r^{22}}(r^{22} - r^{12})},$$

and

$$r_{11} = \frac{(1 - \frac{2\mu_1}{\sigma_1^2}) + \sqrt{(\frac{2\mu_1}{\sigma_1^2} - 1)^2 + \frac{8\lambda}{\sigma_1^2}}}{2},$$
$$r_{12} = \frac{(1 - \frac{2\mu_2}{\sigma_2^2}) + \sqrt{(\frac{2\mu_2}{\sigma_2^2} - 1)^2 + \frac{8\lambda}{\sigma_2^2}}}{2},$$
$$r_{21} = \frac{(1 - \frac{2\mu_1}{\sigma_1^2}) - \sqrt{(\frac{2\mu_1}{\sigma_1^2} - 1)^2 + \frac{8\lambda}{\sigma_1^2}}}{2},$$
$$r_{22} = \frac{(1 - \frac{2\mu_2}{\sigma_2^2}) - \sqrt{(\frac{2\mu_2}{\sigma_2^2} - 1)^2 + \frac{8\lambda}{\sigma_2^2}}}{2}.$$

Proof. First of all, for case 1 ($X \geq l$), we have the fact that the function and its derivative are continuous at point of a, namely

$$a^{r_{12}} = c_1 a^{r_{11}} + c_2 a^{r_{21}}, \tag{8}$$

$$r_{12} a^{(r_{12}-1)} = c_1 r_{11} a^{(r_{11}-1)} + c_2 r_{21} a^{(r_{12}-1)}. \tag{9}$$

By solving equations (8) and (9), we get

$$c_1 = \frac{a^{r^{12}}(r^{21} - r^{12})}{a^{r^{11}}(r^{21} - r^{11})},$$
$$c_2 = \frac{a^{r^{12}}(r^{12} - r^{11})}{a^{r^{21}}(r^{21} - r^{11})}.$$

Recalling Lemma 2, under our model, we have the above result.
On the other hand, for case 2 ($X < l$), we have the fact that the function and its derivative are continuous at point of a, namely

$$a^{r_{21}} = b_1 a^{r_{12}} + b_2 a^{r_{22}},$$

$$r_{21} a^{(r_{21}-1)} = b_1 r_{12} a^{(r_{12}-1)} + b_2 r_{22} a^{(r_{22}-1)}.$$

In a similar way, we have

$$b_1 = \frac{a^{r_{21}}(r_{22} - r_{21})}{a^{r_{12}}(r_{22} - r_{12})},$$
$$b_2 = \frac{a^{r_{21}}(r_{21} - r_{12})}{a^{r_{22}}(r_{22} - r_{12})}.$$

Thus the proof is finished. □

Theorem 4. *The expectation of the first hitting time of Geometric Brownian motion with singular volatility term is infinite, i.e. $\mathbb{E}_x[\tau_l] = \infty$.*

Proof. Recall the Laplace transform expression

$$\mathbb{E}_x[e^{-\lambda\tau_l}] = g(\lambda).$$

Taking the derivative of both sides of this equation with respect to λ have

$$\mathbb{E}_x[-\tau_l e^{-\lambda\tau_l}] = g^{'}(\lambda).$$

Then, as λ approaches 0^+, we have

$$\mathbb{E}_x[\tau_l] = -\lim_{\lambda\to 0^+}\frac{g(\lambda)-g(0)}{\lambda} = -\lim_{\lambda\to 0^+}\frac{f(l)-f(x)}{\lambda f(l)}.$$

Using the L'Hopital's rule implies the result. □

3.2 Numerical results

At first, we observe the change of underlying model and the value of Laplace transform with different l. For numerical results, the common coefficients are

$$a = 7, \mu(t) = \begin{cases} 0.125, & X_t \geq a, \\ 0.15, & X_t < a, \end{cases}$$

$$\sigma(t) = \begin{cases} 1.1, & X_t \geq a, \\ 1.5, & X_t < a, \end{cases} X_0 = 8, \lambda = 0.8.$$

The boundary l are supposed to be $l = 4.5$ and $l = 6.5$, respectively. The Figure 8 & Figure 9 below show the numerical simulation results. In this way, the larger l is, the larger Laplace transform is, the smaller the first hitting time is.

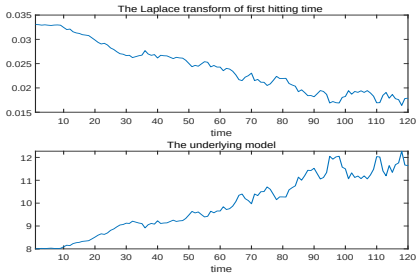

Fig. 8: The figures are the Laplace transform of first hitting time and the underlying model, respectively. The figures rely on $l = 4.5$.

Then, we want to know the change of the underlying model and the value of Laplace transform by changing the value of X_0 by using Matlab. For numerical simulation, let

$$a = 7, \mu(t) = \begin{cases} 0.125, & X_t \geq a, \\ 0.15, & X_t < a, \end{cases}$$

$$\sigma(t) = \begin{cases} 1.1, & X_t \geq a, \\ 1.5, & X_t < a, \end{cases} l = 6.5, \lambda = 0.8.$$

$X_0 = 8$ and $X_0 = 13$ are taken respectively. The Figure 10 and Figure 11 below show the numerical simulation results. In this way, the larger X_0 is, the smaller Laplace transform is, the larger the first hitting time is.

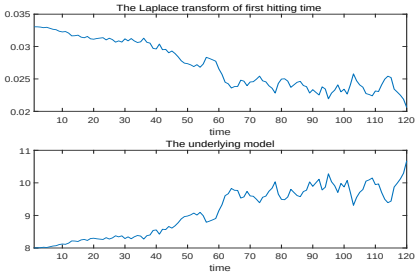

Fig. 9: The figures are the Laplace transform of first hitting time and the underlying model, respectively. The figures rely on $l = 6.5$.

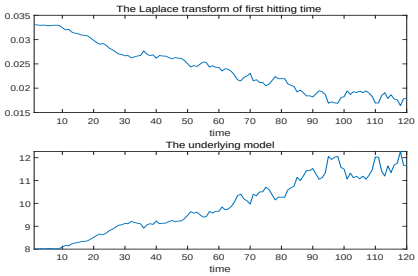

Fig. 10: The figures are the Laplace transform of first hitting time and the underlying model, respectively. The figures rely on $X_0 = 8$.

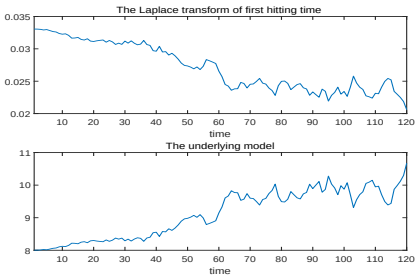

Fig. 11: The figures are the Laplace transform of first hitting time and the underlying model, respectively. The figures rely on $X_0 = 13$.

4 Conclusion

In this paper, the option pricing and Laplace transform of first hitting time problem under Geometric Brownian motion with singular volatility are studied and the numerical simulations are carried out to verify the accuracy of the conclusions. The following conclusions can be drawn:

(i)A rich body of literature on option pricing problem contain complex calculations and numerical results under complex models. Unlike their methods, we adopt probability scheme to directly get the closed-form solution instead of previous methods. In contemporary financial problems, especially in the pricing of path-dependent financial derivatives.

(ii)We use the Sturm-Liouville equation and Euler's formula to get the Laplace transform of the first hitting time. Furthermore, the density of the first hitting time can be deduced by inverse Laplace transform. In order to better depict the financial market, Geometric Brownian motion model has been widely used in the financial field, and there is a large room for improvement. But most of the model are too ideal to make the pricing problem difficult. Hence in our paper we discuss Geometric Brownian motion with singular volatility.

In summary, in the process of deducing option pricing we use probability scheme. In solving Laplace transform of the first hitting time we use the Sturm-Liouville equation and Euler's formula to derive the closed-form solution, and then give some main results. Compared with other numerical results, our solutions are closed-form and accurate.

In the future, we will focus on introducing jump or random volatility and extending our model to the sticky OU or sticky CIR model to reflect more realistic phenomena, but need the density function of the underlying models. This seems to be a big challenge for future study.

References:

[1] V. Stojkoski, Z. Utkovski, L. Basnarkov, L. Kocarev (2019) Cooperation dynamics in networked Geometric Brownian motion. Physical Review E, 99(6):062312.

[2] V. Stojkoski, M. Karbevski, Z. Utkovski, L. Basnarkov, L. Kocarev (2019) Evolution of cooperation in populations with heterogeneous multiplicative resource dynamics. arXiv preprint arXiv:1912.09205.

[3] O. Peters, W. Klein (2013) Ergodicity breaking in Geometric Brownian motion. Physical review letters, 110(10):100603.

[4] V. Stojkoski, T. Sandev, L. Basnarkov, L. Kocarev, R. Metzler (2020) Generalised geometric Brownian motion: Theory and applications to option pricing. arXiv.org, 10.3390.

[5] S. Ross (2014) Introduction to Probability Models-ScienceDirect. Introduction to Probability Models (Eleventh Edition), 2014:iii.Academic Press.

[6] F. Kato, T. Sasaki, K. Narita (2012) A-12-4 Traffic analysis using fractional Geometric Brownian motion and time-varying linear filter. Society Conference of Ieice. The Institute of Electronics, Information and Communication Engineers.

[7] P.J. Ossenbruggen, E.M. Laflamme (2019) Explaining Freeway Breakdown with Geometric Brownian Motion Model. Journal of Transportation Engineering Part A Systems, 145(9):04019037.

[8] N.T. Phong, V. Likhitruangsilp, M. Onishi (2017) Developing a stochastic traffic volume prediction model for public-private partnership projects. S-mart Construction Towards Global Challenges (I-CONBUILD 2017), 1903(1):1-6.

[9] S. Abidin, M. Jaffer (2014) Forecasting Share Prices of Small Size Companies in Bursa Malaysia using Geometric Brownian Motion, Applied Mathematics & Informantion Sciences, 8(1):107-112

[10] M. Lefebvre (2010) Geometric Brownian motion as a model for river flows. Hydrological Processes, 16(7):1373-1381.

[11] L. Fan (1998) The value of investment opportunity and investment decision-Geometric Brownian motion model. Journal of Systems Engineering, 1998(3):8-12.

[12] N.J. Cutland, P.E. Kopp, W. Willinger (1991) Nonstandard methods in option pricing. IEEE Conference on Decision & Control IEEE.

[13] Y. Hsu, P. Chen, C. Wu (2022) Double-barrier option pricing equations under extended geometric Brownian motion with bankruptcy risk. Statistics & Probability Letters 184:109383.

[14] R. Delpasand, M. Hosseini (2023) Numerical solution of the three-asset Black–Scholes option pricing model using an efficient hybrid method. Stochastics and Dynamics, 14(02):2350035.

[15] C. Liu, S. Zhu, S. Zhang (2023) Pricing double-barrier Parisian options. IMA Journal of Management Mathematics, 34(4):633-660.

[16] K. Kazmi (2023) A second order numerical method for the time-fractional Black–Scholes European option pricing model. Journal of Computational and Applied Mathematics, 418:114647.

[17] T. Arai (2023) Deep learning-based option pricing for Barndorff–Nielsen and Shephard model. International Journal of Financial Engineering, 10(03):2350015.

[18] P.A. Samuelson (2015) Proof that Properly Anticipated Prices Fluctuate Randomly. World Scientific Book Chapters, 6(2):25-38.

[19] F. Black, M.S. Scholes (1973) The Pricing of Options and Corporate Liabilities. Journal of Political Economy, 81(3):637-654.

[20] R.C. Merton (1973) Rational theory of option pricing. The Bell Journal of Economics and Management Science, 4(1):141-183.

[21] J. Cox, S. Ross, M. Rubinstein (1979) Option pricing: A simplified approach. Journal of Financial Economics, 7(3): 229-263.

[22] G. Bakshi, C. Cao, Z. Chen (1997) Empirical Performance of Alternative Option Pricing Models. The Journal of Finance, 52(5):1765-2223.

[23] D. Duffie, J. Pan, K. Singleton (2000) Transform Analysis and Asset Pricing for Affine Jump-diffusions. Econometrica, 68(6): 1343-1376.

[24] J. Zhu (2009) Testing for expected return and market price of risk in Chinese A and B share markets: A Geometric Brownian motion and multivariate GARCH model approach. Mathematics & Computers in Simulation, 79(8):2633-2653.

[25] D. Delpini (2010) Modeling and analysis of financial time series beyond Geometric Brownian motion. Scientifica Acta 4(1):15-22.

[26] S. Song, G. Xu, Y. Wang (2016) On First Hitting Times for Skew CIR Processes. Methodology & Computing in Applied Probability, 18(1):1-12.

[27] J. Zhong (2015) Research on the first arrival time of Regime Switching geometric Brownian motion process and its application in finance and insurance. East China Normal University.

[28] H. Zhang, P. Jiang (2021) On some properties of sticky Brownian motion. Stochastics and Dynamics, 21(06):2150037.

[29] H. Zhang, Y. Tian (2023) Hitting times for sticky skew CIR process. Stochastics, DOI: 10.1080/17442508.2023.2255341.

[30] E. Mordecki, P.H. Salminen (2019) Optimal stopping of Brownian motion with broken drift. High Frequency, 2(2):113-120.

[31] A.N. Borodin, P. Salminen (1996) Handbook of brownian motion-facts and formulae. Journal of the American Statistical Association, 93(442):657-658.

Contribution of Individual Authors to the Creation of a Scientific Article (Ghostwriting Policy)

Haoyan Zhang proposed the idea of the method and checked the correctness of the manuscript. Yece Zhou gave the method and calculated the option price. Xuan Li wrote the article and provided the numerical results. Yinyin Wu computed the first hitting time problem and polish the language.

Sources of Funding for Research Presented in a Scientific Article or Scientific Article Itself

This work is supported by the National Natural Science Foundation of China (No.12101602).

Conflict of Interests

The authors declare that there is no conflict of interests regarding the publication of this paper.